Determination of the Primordial Magnetic Field Power Spectrum by Faraday Rotation Correlations

Tsafrir Kolatt[1]

Harvard-Smithsonian Center for Astrophysics, 60 Garden St., Cambridge, MA 02138

and

The Physics Department and Lick Observatory, UCSC, Santa-Cruz, CA 95064

ABSTRACT

This paper introduces the formalism which connects between rotation measure (RM) measurements for extragalactic sources and the cosmological magnetic field power spectrum. It is shown that the amplitude and shape of the cosmological magnetic field power spectrum can be constrained by using a few hundred radio sources, for which Faraday RMs are available. This constraint is of the form $B_{rms} \lesssim 1 \times [2.6 \times 10^{-7} \text{cm}^{-3}/\bar{n}_b]h$ nano-Gauss (nG) on $\sim 10 - 50$ h^{-1}Mpc scales, with $\bar{n}_b$ the average baryon density and h the Hubble parameter in 100 km s^{-1} Mpc^{-1} units. The constraint is superior to and supersedes any other constraint which come from either CMB fluctuations, Baryonic nucleosynthesis, or the first two multipoles of the magnetic field expansion. The most adequate method for the constraint calculation uses the Bayesian approach to the maximum likelihood function. I demonstrate the ability to detect such magnetic fields by constructing simulations of the field and mimicking observations. This procedure also provides error estimates for the derived quantities.

The two main noise contributions due to the Galactic RM and the internal RM are treated in a statistical way following an evaluation of their distribution. For a range of magnetic field power spectra with power indices $-1 \leq n \leq 1$ in a flat cosmology (Ω_m=1) we estimate the signal-to-noise ratio, Q, for limits on the magnetic field B_{rms} on ~ 50 h^{-1}Mpc scale. Employing one patch of a few square degrees on the sky with source number density n_{src}, an approximate estimate yields $Q \simeq 3 \times (B_{rms}/1\text{nG})(n_{src}/50 \deg^{-2})(2.6 \times 10^{-7}\text{cm}^{-3}/\bar{n}_b) h$. An all sky coverage, with much sparser, but carefully tailored sample of ~ 500 sources, yields $Q \simeq 1$ with the same scaling. An ideal combination of small densely sampled patches and sparse all-sky coverage yields $Q \simeq 3$ with better constraints for the power index. All of these estimates are corroborated by the simulations.

Subject headings: Cosmology: Large-Scale Structure of Universe, Theory – Magnetic Fields – Polarization – Methods: Statistical

---

[1]email:tsafrir@physics.ucsc.edu

1. INTRODUCTION

There is plenty evidence for magnetic fields on the scale of the earth, the solar system, the interstellar medium, galaxies and clusters of galaxies [for the extragalactic magnetic field see review by Kronberg (1994, K94) and references therein]. We still don't know however whether any larger scale magnetic fields exist. There are various upper limits on the rms value of the cosmological magnetic field, but the upper limits are still too high to exclude any relevance to magnetic fields observed on smaller scales. Cosmological magnetic fields might help to resolve the bothersome question of the origin of the $\sim 10^{-6}$G magnetic field which exists on galactic scales or fields of similar size seen on the scales of galaxy clusters. A primordial (pre – galaxy formation) magnetic field amplified by the gravitational collapse, and then by processes like differential rotation and dynamo amplification (Parker 1979), can serve to seed these observed smaller scale magnetic fields.

The most stringent upper limits to date for magnetic fields on cosmological scales come from three different sources:

1. Big Bang Baryonic Nucleosynthesis (BBN).

   Magnetic fields that existed during the BBN epoch would affect the expansion rate, the reaction rates, the electron density (and possibly the space-time geometry). By taking all these effects into account in the calculation of the element abundances, and then comparing the results with the observed abundances one can set limits on the magnetic field amplitude. The limits for homogeneous magnetic fields on scales $\gg 10^{-14}$ h^{-1}Mpc (distances are quoted in comoving coordinates) and up to the BBN horizon size ($\sim 10^{-4}$ h^{-1}Mpc) are $10^{-9} - 10^{-6}$ G in terms of today's values (Grasso & Rubinstein 1995, 1996 ; Cheng, Olinto, Schramm, & Truran 1996). The relevance of these limits for the maximum value of magnetic field seeds on the subgalactic scale is obvious, but in order for these limits to be relevant to the intergalactic magnetic field, further assumptions about the super-horizon magnetic field power spectrum and the magnetic field generation epoch should be made.

2. The CMB radiation.

   The presence of magnetic fields during the time of decoupling causes anisotropy, *i.e.* different expansion rates in different directions (Zel'dovich & Novikov 1975). Masden (1989) provides a useful formula for the connection between the measured temperature fluctuations on a given scale at z_d, the decoupling time, and the limits on the equivalent scale today. For a magnetic field energy density much smaller than the matter energy density, the limit is

   $$B_{rms}(R) \leq 3 \times 10^{-4} h \frac{\sqrt{\frac{\Delta T}{T}(R)\Omega}}{\sqrt{1+z_d}} \ \text{G} . \tag{1}$$

   For typical values of $h = 1$ (the Hubble constant in units of 100 km s^{-1} Mpc^{-1}), temperature fluctuations of $\sim 10^{-5}$, $\Omega = 1$ and $z_d \simeq 10^3$ the limit becomes $B_{rms} < 10^{-8} - 10^{-9}$G. Recently, Barrow, Frreira, & Silk (1997) used the COBE 4-year data to constrain the magnetic field on the horizon scale by $B(R = R_h) < 6.8(\Omega h^2)^{1/2}$ nG.

3. Multipole expansion of RM observations.

Passing through a magnetoionic medium, polarized light undergoes rotation of the polarization vector (Faraday rotation, for definition see §2). The rotation amount is proportional to the dot product of the magnetic field and the light propagation direction, and to the distance the light travels through the medium. If any cosmological magnetic field exists, the farther away the source, the more the polarized light component is rotated. We refer to this as the "monopole" term. This term exists even if the field has no preferred direction on the horizon scale, namely even without breaking the isotropy hypothesis.

If there is a preferred direction to the field on a cosmological scale, a dipole will show up in the RM measurements across the sky, due to the different sign of the dot product (and thus the different rotation direction). So far attempts have been made only to identify a monopole or a dipole in the magnetic field for scales of $z \simeq 2.5$ (Kronberg 1976) and $z \simeq 3.6$ (Vallée 1990). The search for a dipole signature in the Faraday rotation values for a sample of extragalactic sources (QSO) yields limits of $B < 1 - 10^{-1}$ nG depending on the assumed cosmology (Kronberg & Simard-Normandin 1976, Kronberg 1976). Vallée (1990) tried to estimate the limits on the dipole and the monopole terms and concluded that an all-prevailing (up to $z = 3.6$) field must be smaller than $6 \times 10^{-2} \left[\frac{10^{-6} \text{cm}^{-3}}{\bar{n}_b} \right]$ nG .

Other potential methods of detecting a possible cosmological magnetic field include distortion of the acoustic ("Doppler") peak in the CMB power spectrum (Adams, Danielsson, Grasso, & Rubinstein 1996) and Faraday rotation of the CMB radiation polarized components (Loeb & Kosowsky 1996). These methods where not designed to probe any magnetic field generated after recombination. Their implementation is still pending on the upcoming measurements of the CMB fluctuations and polarization.

A method that does probe magnetic fields generated in the post recombination era, relies on cosmic ray (CR) detection. The effect of magnetic fields on high energy CRs ($> 10^{18}$ eV) is twofold. It will first alter the energy distribution of CRs (Lee, Olinto, & Sigl 1995, Waxman & Miralda-Escudé 1996) and then, if the CR direction is identified and attributed to a known region or source, the magnetic field either smears the directionality (for field coherent scales much smaller than the distance to the source) or deflects the CR direction from aligning with the source direction. Current limits from this last effect are either very weak or non-existing.

Theories for primordial magnetic fields in the framework of structure evolution paradigms have been suggested by a number of authors. Magnetic fields on cosmological scales emerge in the framework of these theories in one of three epochs: the inflation era, the plasma era, and the post-recombination era. In the inflation era, magnetic fields form due to quantum mechanical processes (Turner & Widrow 1988; Quashnock, Loeb, & Spergel 1989, Vachaspati 1991, Ratra 1992a, 1992b, Dolgov & Silk 1993) or possibly magneto-hydrodynamics (Brandenburg, Enquist, & Olesen 1996). During the plasma era, prior to recombination, magnetic fields form due to vorticity caused by the mass difference between the electron and the proton (Harrison 1973, but see Rees 1987), or where magnetic field fluctuation survival (no vorticity assumed) depends on the fluctuation scale

(Tajima *et al.* 1992). Other authors have pointed out that even in the post recombination era (but before galaxy formation) magnetic fields can be generated by tidal torques (Zweibel 1988), or by cosmic strings wakes (Ostriker & Thompson 1987, Thompson 1990). Magnetic field generated in the process of structure formation itself, due to falling matter (Pudritz & silk 1989), or star burst regions, are less likely to feed back into the intergalactic space and to affect the cosmological magnetic field. Nevertheless, proposals in this spirit were also considered by taking into account wind driven plasma which fills intergalactic space with magnetic fields.

Whatever the origin of cosmological magnetic fields, each suggested theory, specifies the magnetic field amplitude and power spectrum shape. Thus, each of the theories can in principle become refutable if we could measure, or put limits on, the normalized power spectrum of the cosmological magnetic field.

This challenge and the realization that with existing or upcoming data, it will be possible to measure the magnetic field power spectrum has led us to develop a method for doing so. We argue that much better estimates (or upper limits) for the cosmological magnetic field can be calculated by using the RM correlation matrix.

All previous attempts to limit the cosmological magnetic field dipole on very large scales ($z \simeq 2.5 - 3.6$), suffer from two drawbacks. From a theoretical point of view it is difficult to reconcile the necessary anisotropy such a dipole imposes with other evidence which suggest global isotropy. From a practical point of view, this test is confined to one scale, and doesn't allow measurements over a whole range. Only by extending the measurement to a whole range, can one estimate the full power spectrum (PS). Although contribution from a "random walk" can be useful even if only a monopole is calculated (see below), the information is partial, inferior to the full derivation of the magnetic field by RM correlations, and sensitive to evolutionary effects.

Why is the correlation approach more advantageous than other type of statistics and in particular why is it better than the monopole approach? In the monopole approach we are looking for a correlation between RM values and the source redshift. Let's pretend at first that all measurements are exact and there are no noise sources (we'll notice in §3 that these two assumptions are far too optimistic). Consider a scale l_0 over which the magnetic field is coherent with an rms value of B_{rms}. A line-of-sight to a source at a distance r_{src} will cross $N_l = r_{src}/l_0$ such regions. There is no correlation in the magnetic field orientation between the regions, and on average each one of them contributes $\mathrm{RM}^i_{rms} \propto B_{rms}l_0$. The overall contribution due to N_l random walk steps sums up to $\mathrm{RM}_{rms} = \sqrt{N_l}\mathrm{RM}^i_{rms} \propto B_{rms}\sqrt{l_0 r_{src}}$. It is thus clear that the larger r_{src}, the bigger RM_{rms} we expect for an ensemble of sources located at r_{src}. Now let's turn to the correlation approach. Two lines-of-sight to two adjacent sources (separation angle γ and assume the same redshift for the two) are observed for correlation between the RM values of the polarized light emanating from them. If $\gamma r_{src} \leq l_0$ the two light rays undergo *the same* rotation in each patch of length l_0 (for small γ we neglect the difference in the $\cos(\theta)$ term between the magnetic field and the line-of-sight). The ensemble average of the correlation term would then be $< \mathrm{RM}_1\mathrm{RM}_2 >^{1/2} = N_l\mathrm{RM}^i_{rms} \propto B_{rms}r_{src}$, with the same proportionality constant as before. In the limit of $l_o \to r_{src}$, the two expressions

coincide, but for any value of $l_0 < r_{src}$, the signal from the correlation calculation is amplified by the factor $\sqrt{r_{src}/l_0}$. For example, if $r_{src} = 1700$ h^{-1}Mpc ($z \simeq 1$) and $l_0 = 10$ h^{-1}Mpc the signal is amplified by more than an order of magnitude. Moreover, the correlation provides information about the power spectrum (different γ and r_{src} values) of the magnetic field that otherwise we wouldn't be able to obtain. The correlation also makes it easier to separate the noise from the signal, unlike the monopole approach. We will return to this approximation later on, under more realistic considerations (§3.5), when we attempt to evaluate the number of pairs needed in order to establish a certain signal-to-noise ratio at a given scale (γ). For now, this simple model demonstrates the advantages of this paper's approach.

In order to relate actual data of RM measurements to the magnetic field, we begin by considering the connection between the two. In section 2 we introduce the magnetic field correlation tensor and its connection to the RM correlation. In section 3 we make use of these definitions and describe the calculation procedure for the RM correlation from the raw data to the constraints on the magnetic field power spectrum. A key issue is the estimate of noise from non-cosmological contributions to the RM. The impatient reader can turn immediately to §3.5 to get a rough estimate for the expected signal-to-noise ratio. We demonstrate the procedure in the following section (§4), where we simulate a few realistic examples of cosmological magnetic fields, and exploit them to get RM measurements from which we derive back an estimate for the original power spectrum. The simulations also allow us to perform a realistic error analysis. In section 5 we discuss prospects for applying the procedure to real data and conclude with our results.

2. THE ROTATION MEASURE CORRELATION MATRIX

Linearly polarized electro-magnetic radiation of frequency ν traveling a distance dl through a non-relativistic plasma medium with the magnetic field $\vec{B}$, is rotated by the angle dϕ. In other words, the polarization angle is changed by (*e.g.* Lang 1978 Eqs. 1-268 $-$ 1-270)

$$d\phi = \frac{e^3 n_e}{2\pi m_e^2 \nu^2} \vec{B} \cdot \vec{dl} \, , \tag{2}$$

where e, m_e, and n_e are the electron charge, mass, and number density respectively (we use units of $c = 1$). The rotated polarization vector itself is written

$$p(\nu) = |p(\nu)| e^{2i\phi} \, , \tag{3}$$

a pseudo-vector degenerated in rotation of ϕ by $n\pi$. It is related to the Stokes parameters via

$$|p| = \frac{(Q^2 + U^2)^{1/2}}{I} \, ; \qquad \phi = \frac{1}{2} \tan^{-1} \left(\frac{U}{Q} \right) \, , \tag{4}$$

that in turn are expressed by the electric field components perpendicular to the wave propagation direction (z)

$$I = E_x^2 + E_y^2$$

$$Q = E_x^2 - E_y^2$$
$$U = E_y^* E_x + E_y E_x^* \tag{5}$$

where time average is explicitly assumed.

In the cosmological context, some of the quantities are functions of time (or equivalently redshift or distance). We assume fully ionized gas (ionization fraction $X_e = 1$) and thus the average number density of free electrons is

$$\bar{n}_e = X_e \bar{n}_b = \bar{n}_b. \tag{6}$$

The baryon number density at a specific location is $n_b(\vec{x}) = \bar{n}_b(1+\delta(\vec{x}))$, with $\delta(\vec{x})$ the dimensionless density fluctuation. Number densities scale like a^{-3}, where a is the scale factor. The frequency scales like a^{-1}, and under the assumption of flux conservation, B scales like a^{-2}. The distance unit "dl" in a Robertson-Walker metric is given by

$$dl = dt = a(t)d\eta = \frac{dr}{\sqrt{1 - Kr^2}}, \tag{7}$$

expressed via η the conformal time. Since $a = (1 + z)^{-1}$ for the redshift z, the overall rotation of the polarized radiation of a source at the redshift z, the direction $\hat{q}$ as observed from $\vec{x}$, (we set $x = 0$ for simplicity) and at frequency ν_0, is given by

$$\int_0^r d\phi = \frac{e^3 \bar{n}_{b_0}}{2\pi m_e^2 \nu_0^2} \int_0^{r(z)} [1 + \delta(\hat{q}r')] (1 + z')^3 \vec{B}_0(\hat{q}r') \cdot \hat{q} \frac{dr'}{\sqrt{1 - Kr'^2}} = \frac{RM(\hat{q}, z)}{\nu_0^2}. \tag{8}$$

Today's values are all denoted by the subscript "0" and $z' = z(r')$. The time dependence of $\delta(\hat{q}r')$ is taken into account later on (*cf.* Eq. 12). The two point correlation function of the RM is defined by

$$\Upsilon \equiv \langle RM(\hat{q}_1, z_1) RM(\hat{q}_2, z_2) \rangle, \tag{9}$$

see Nissen & Thielheim (1975) for a similar definition. Throughout the paper, $\langle ... \rangle$ is the notation for an ensemble average. We use the notation $\vec{r}' = \vec{r}_1{}' - \vec{r}_2{}'$ and obtain

$$\Upsilon = \left(\frac{e^3 \bar{n}_{b_0}}{2\pi m_e^2}\right)^2 \int_0^{r_1(z_1)} \frac{dr_1'}{\sqrt{1 - Kr_1'^2}} [1 + \delta(\hat{q}_1 r_1')] (1 + z_1')^3 \int_0^{r_2(z_2)} \frac{dr_2'}{\sqrt{1 - Kr_2'^2}} [1 + \delta(\hat{q}_2 r_2')] (1 + z_2')^3$$

$$\times \hat{q}_{1i} \hat{q}_{2j} \frac{1}{V} \int B_{0i}(\vec{x}) B_{0j}(\vec{x} + \vec{r}') d^3\vec{x}, \tag{10}$$

where summation over the spatial components i, j is assumed. The integral (10) is made out of four terms. Two of the terms (those involve only one power of δ) vanish because $\langle \delta \rangle = 0$ and we assume vanishing correlation between the density fluctuations and magnetic fluctuations $[\langle \vec{B}(\vec{x})\delta(\vec{x} + \vec{r}) \rangle = 0 \, \forall(\vec{x}, \vec{r})]$ due to the vector nature of $\vec{B}$ and the scalar δ.

The two remaining terms are

$$\Upsilon_0 = \left(\frac{e^3 \bar{n}_{b_0}}{2\pi m_e^2}\right)^2 \int_0^{r_1(z_1)} \frac{dr_1'}{\sqrt{1 - Kr_1'^2}} (1 + z_1')^3 \int_0^{r_2(z_2)} \frac{dr_2'}{\sqrt{1 - Kr_2'^2}} (1 + z_2')^3 \times$$

$$\hat{q}_{1i}\hat{q}_{2j}\frac{1}{V}\int B_{0i}(\vec{x})B_{0j}(\vec{x}+\vec{r}')\mathrm{d}^3\vec{x}\,, \tag{11}$$

and

$$\Upsilon_\xi = \left(\frac{e^3\bar{n}_{b_0}}{2\pi m_e^2}\right)^2 \int_0^{r_1(z_1)} \frac{\mathrm{d}r_1'}{\sqrt{1-Kr_1'^2}}(1+z_1')^2 \int_0^{r_2(z_2)} \frac{\mathrm{d}r_2'}{\sqrt{1-Kr_2'^2}}\xi_0(\vec{r}')(1+z_2')^2\times$$

$$\hat{q}_{1i}\hat{q}_{2j}\frac{1}{V}\int B_{0i}(\vec{x})B_{0j}(\vec{x}+\vec{r}')\mathrm{d}^3\vec{x}\,, \tag{12}$$

where $\xi(r)$ is the baryonic matter correlation function that we identify with the matter correlation function. Today's value of it is ξ_0 and the missing powers of $(1+z)$ in Eq. (12) account for the linear evolution of this correlation. The RM correlation function is the sum $\Upsilon = \Upsilon_0 + \Upsilon_\xi$.

The last integral of Eqs. (10, 11, 12) is the correlation tensor of the magnetic field defined as $C_{ij}(\vec{r}) = \langle B_i(\vec{x})B_j(\vec{x}+\vec{r})\rangle$. In the cosmological case, we assume isotropy on scales much smaller than the horizon and confine C_{ij} to be a function of $|\vec{r}|$ only. Being a divergence-free field the magnetic field correlation can be written (Monin & Yaglom 1975) as a combination of parallel ($C_\parallel$) and perpendicular ($C_\perp$) functions. The parallelism and orthogonality are given with respect to the connecting vector: $\vec{r} = \vec{r}_1 - \vec{r}_2$

$$C_{ij}(\vec{r}) = [C_\parallel(r) - C_\perp(r)]\frac{r_ir_j}{r^2} + C_\perp(r)\delta_{ij}^K\,,$$

$$C_{jl}(\vec{k}) = \int C_{jl}(\vec{r})\,\exp(-i\vec{k}\cdot\vec{r})\,d^3r$$

$$C_{jl}(\vec{k}) = [C_\parallel(k) - C_\perp(k)]\frac{k_jk_l}{k^2} + C_\perp(k)\delta_{jl}^K\,, \tag{13}$$

where δ_{ij}^K is the Kronecker δ-function. In the spectral domain we define the function $E(k) = 4\pi k^2 C_\perp(k)$ and express both correlation functions by the function $E(k)$, namely

$$C_\perp(r) = \int_0^\infty \mathrm{d}kE(k)\left(j_0(kr) - \frac{j_1(kr)}{kr}\right) \quad ; \quad C_\parallel(r) = 2\int_0^\infty \mathrm{d}kE(k)\frac{j_1(kr)}{kr}\,, \tag{14}$$

with j_i denoting the spherical Bessel function of the ith order. When people refer to the "magnetic power spectrum" they usually mean $C_\perp(k)$ which should further be multiplied by k^2 in order to get $E(k)$. We shall hereafter comply with this notation and refer to $C_\perp(k)$ as the three-dimensional "magnetic power spectrum", $P_B(k)$. Figure 1 show the two functions $C_\parallel(r)$ and $C_\perp(r)$ in units of $C_\perp(0)$ for three values of the power index $n = -1, 0, 1$ [$P_B(k) \propto k^n$]. Each function is shown with a minimal Gaussian smoothing of 1.5 h^{-1}Mpc. Naturally, smaller power indices mean larger correlation length.

Going back to the expression (10) for the RM correlation we can rewrite it as

$$\Upsilon_0 = \left(\frac{e^3\bar{n}_{b_0}}{2\pi m_e^2}\right)^2 \int_0^{r_1(z_1)} \frac{\mathrm{d}r_1'}{\sqrt{1-Kr_1'^2}}(1+z_1')^3 \int_0^{r_2(z_2)} \frac{\mathrm{d}r_2'}{\sqrt{1-Kr_2'^2}}(1+z_2')^3\times$$

$$\left\{[C_\parallel(r') - C_\perp(r')](\hat{q}_1\cdot\hat{r}')(\hat{q}_2\cdot\hat{r}') + C_\perp(r')\hat{q}_1\cdot\hat{q}_2\right\}\,. \tag{15}$$
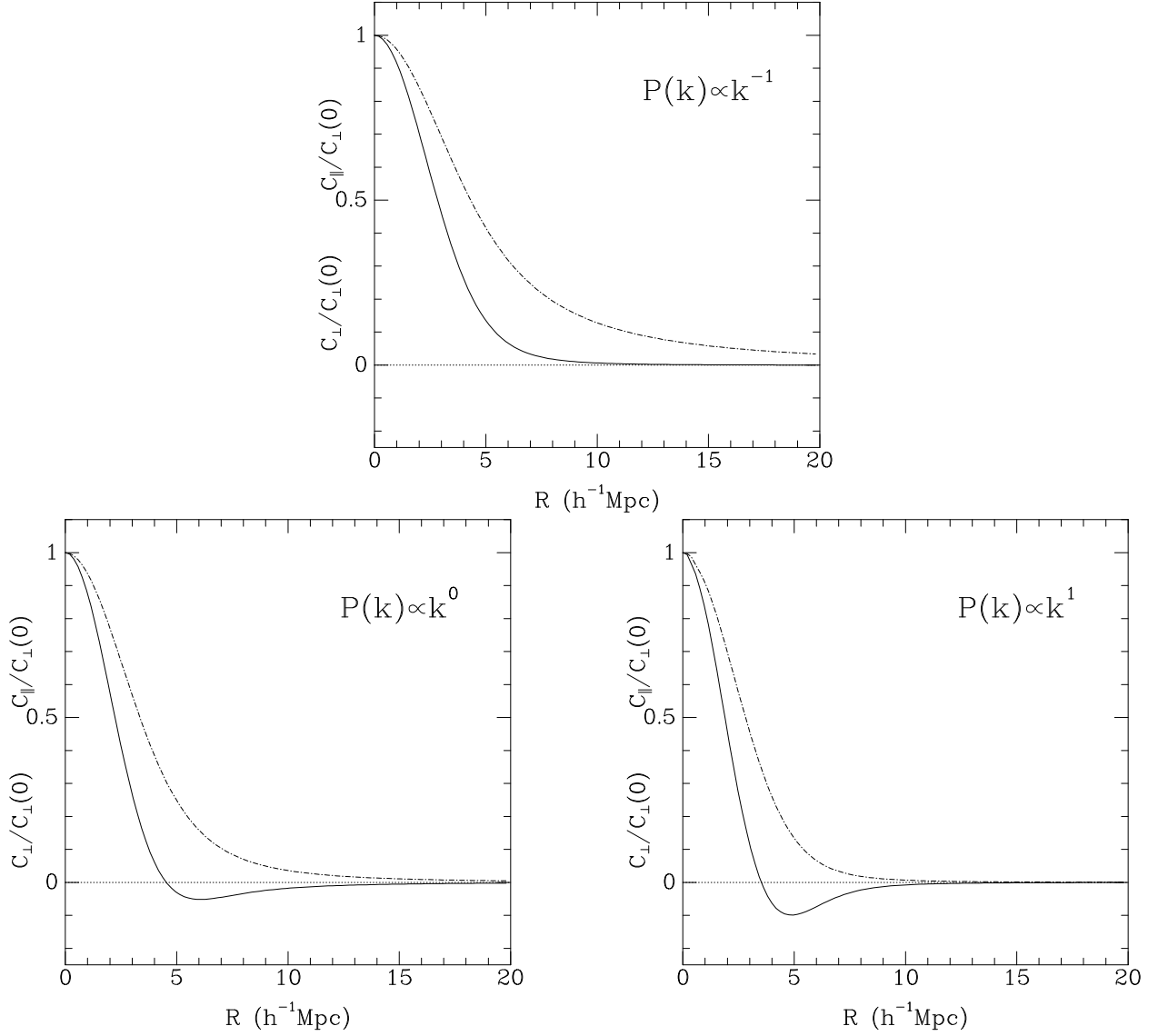
Fig. 1.— The parallel (dotted-dashed line) and perpendicular (solid line) components of the magnetic field correlation tensor. Units are of $C_\perp (= C_\parallel)$ in the origin. Plotted are three cases: (a) $P_B(k) \propto k^{-1}$, (b) $P_B(k) = const.$, (c) $P_B(k) \propto k$. Gaussian smoothing of 1.5 h^{-1}Mpc applied.

As expected, the RM correlation depends only on the relative distance, $|\vec{r}|$, and the angle.

For comoving distances between two sources at z_1 and z_2 separated by the angle γ on the sky we use Weinberg's (1972, Eq. 14.2.7) coordinate transformation, implemented by Osmer (1981) for the $q_0 = 0$ case (q_0 – the deceleration parameter) and generalized by Boyle (1986) for other q_0 values. For the flat universe case ($q_0 = 0.5$) the comoving relative distance reduces to the simple

form

$$r(z_1, z_2, \gamma) = \frac{1}{H_0} \left[r_1(z_1)^2 + r_2(z_2)^2 - 2r_1(z_1)r_2(z_2)\cos\gamma \right]^{1/2} . \tag{16}$$

The distance to a source at the redshift z (no cosmological constant) is given by (Kolb & Turner 1990, Eq. 3.112)

$$r(z) = \frac{1}{H_0} \frac{2\Omega_0 z + (2\Omega_0 - 4)(\sqrt{\Omega_0 z + 1} - 1)}{\Omega_0^2(1+z)} , \tag{17}$$

and can be easily generalized for other cases.

In order to estimate the importance of Υ_ξ [Eq. (12)] we adopt the APM power spectrum (Baugh & Efstathiou 1993; Tadros & Efstathiou 1995) with the fitting formula

$$P_m(k) = \frac{2\pi^2}{k^3} \frac{(k/k_0)^{3-m}}{1 + (k/k_c)^{-(m+n)}} , \tag{18}$$

the fitting parameters $m = 1.4$, $k_c = 0.02$, $k_0 = 0.19$, and Gaussian smoothing of 1.5 h^{-1}Mpc. We then derive the real space correlation function by the Fourier transform of the smoothed power spectrum. In the range $3 - 30$ h^{-1}Mpc the result is very similar to the derived APM real space correlation function (no explicit smoothing) $\xi_0 = (r/5.25 \ h^{-1}\text{Mpc})^{-1.7}$ (Baugh 1995). For this choice we get (regardless of the $P_B(k)$ form, and for $z_{src} \gtrsim 0.5$), $|\Upsilon_\xi/\Upsilon| < 10^{-4}$. We hence identify $\Upsilon = \Upsilon_0$ hereafter.

2.1. The Power Spectrum Normalization

We relate the magnetic field normalization to the power spectrum by $B_{rms}(R)$ where

$$(B_{rms}^{G,TH})^2(R) = \frac{3}{2\pi^2} \int_0^\infty P_B(k)k^2 W_{G,TH}^2(kR)\mathrm{d}k , \tag{19}$$

the factor 3 is due to the definition of $P_B(k)$ [as $C_\perp(r)$], and $W_{G,TH}(kR)$ is the Gaussian (Top-hat) window function of radius R, in k space,

$$W_G = \exp\left[-\frac{(kR)^2}{2}\right] ; \quad W_{TH} = \frac{3}{(kR)^3}[\sin(kR) - kR\cos(kR)] . \tag{20}$$

A good benchmark to use for the normalization range is the CMB limit due to its simplicity and the availability of $\Delta T/T$ measurements on many scales (either today or in the near future). We therefore work in the range of ~ 1 nG throughout this paper.

The observational limits on the magnetic field as deduced from the RM dipole [$R \simeq r(z = 2.5)$ or $R \simeq r(z = 3.6)$] are thus very different from the limits imposed by CMB fluctuations on $1'$ scale. We note that by Eq. (19) one cannot infer limits on the magnetic field magnitude from one scale to another. The limits must involve the power spectrum shape. Since no estimate for the latter exists, and since theoretical predictions for it range from power index of $n = -3$ to $n = 2$ (Ratra 1992a), limits on one particular scale hardly limit other scales.
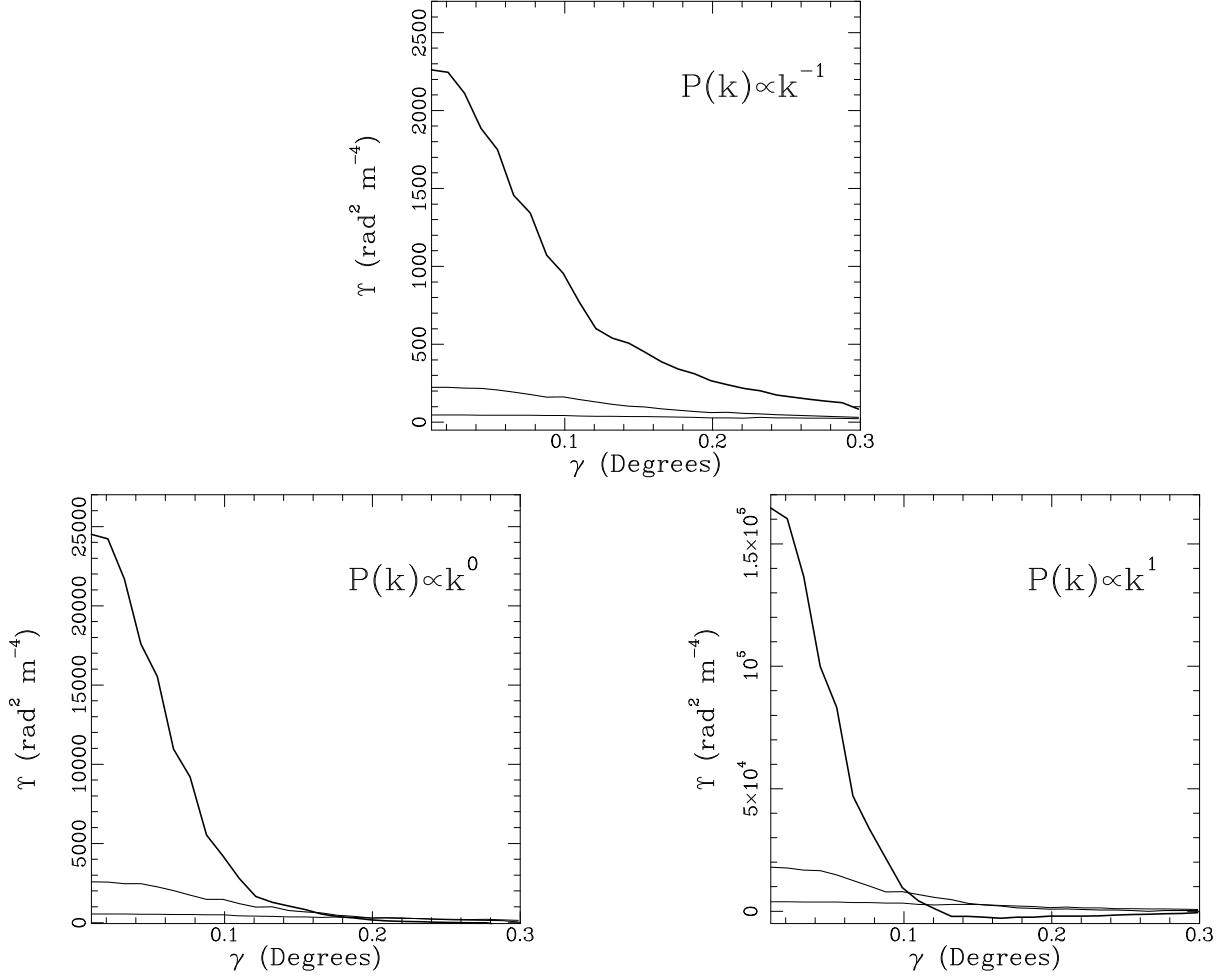
Fig. 2.— RM correlation as function of the separation angle between source pairs at three different redshifts. The redshift values are $z_{src} = 0.5, 1, 2$ with thicker lines for higher redshift. The magnetic field normalization in all cases is $B_{rms}^{TH}(50 \ h^{-1}\mathrm{Mpc}) = 1$ nG . Three magnetic power spectra are shown with the power indices $n = -1, 0, 1$. Note the different y axis scales.

Figure 2 show the values for the RM correlation function for pairs of sources at the same redshift, and three different spectral indices. The normalization of the magnetic field in each case is $B_{rms}^{TH}(50 \ h^{-1}\mathrm{Mpc}) = 1$ nG ($\Omega_m = 1, h = 1, \Omega_b = 0.024$). This scale resembles the mean separation between rich clusters.

We notice that for close pairs, high redshift sources are preferable in order to get high signal, while a transition typically occurs at a fraction of a degree where it becomes preferable to use lower redshift sources. This transition is due to the uncorrelated magnetic fields experienced by high redshift sources with large separation. Only when the two lines-of-sight approach the correlation length, does contribution to the RM correlation becomes substantial. The different, uncorrelated

magnetic fields up to the correlation length, play the role of uncorrelated noise, and dominate the correlated signal from the low redshift segment of the line-of-sight.

On the scale $0.5° - 2.5°$, the RM correlation signal still stands on $\sim 10 - 10^2 \, \text{rad}^2 \, \text{m}^{-4}$ depending on the power spectrum.

3.   CALCULATION PROCEDURE FOR THE CORRELATION MATRIX

3.1.   The Raw Data

The raw data consist of N_{src} extra Galactic objects for which polarization measurements are available in N_λ wavelengths. Broten, Macleod, & Vallée (1988), and Oren & Wolfe (1995) have emphasized the need for a careful selection of wavelengths for each observed source. For the current application there are additional special requirements that will become clear when we get to the discussion (§5).

Each of such N_λ measurements consists of two types of data : the degree of polarization, and the polarization position angle [$|p|$ and 2ϕ of Eq. (3)]. Two functions are then constructed which give the dependence of these on wavelength. The RM is computed from the latter by using Eq. (3) where $\text{RM} = \phi \, \lambda^{-2}$. Each measured RM_m value has an error, ϵ_m, that emerges from the measurement error (instrumental, ionosphere model, the earth magnetic field model etc.) and translates to the error in the fit from which the RM is derived. For typical sources with polarization degree of $\gtrsim 10\%$ (namely $10^{-1} - 10^{-2}$ Jy of polarized component at a few GHz frequency), the measurement error in each datum is of the order of a few degrees (*e.g.* Kato, Tabara, Inoue & Aizu 1987; Simard-Normandin, Kronberg, Button, 1980 (SKB); Oren & Wolfe 1995). For realistic $N_\lambda = 4$, this instrumental error translates to a typical error in the $\phi - \lambda^2$ fit of $0.5 - 5 \, \text{rad} \, \text{m}^{-2}$ and is dwarfed by other noise terms in the procedure (*cf.* §3.2, §3.3). We therefore set $\epsilon_m \simeq 0$ from now on.

The measured RMs are the sum of a few contributions, and cannot be directly plugged into the expression (15) to evaluate Υ.

To begin with, there exists the internal RM_I for every one of the N_{src} extragalactic sources. Then there is the integrated RM_c which is presumably due to the cosmological magnetic field (and the free electrons) along the line-of-sight to the source. There may also exist contribution RM_f from intervening systems along the line-of-sight (foreground screen) either next to the source itself (*e.g.* the host galaxy of a quasar), Lyman-α systems, galaxies, or clusters of galaxies. Before this combined signal gets to the detector it still has to go through the Galactic magnetic field, where it is rotated once more by the amount RM_G. The final measurement, RM_m is thus the linear sum

$$RM_m(\vec{z}_i) = \text{RM}_I^i + \text{RM}_c(\vec{z}_i) + \text{RM}_f(\vec{z}_i) + \text{RM}_G(\hat{z}_i) , \qquad (21)$$

where $\vec{z}_i$ is the redshift-vector [actually translated to a distance vector (*cf.* §2)] for the ith source. Since we are interested in the cosmological contribution to the RM [*i.e.* the second term in Eq. (21)], the first step should involve "cleaning" the measured signal of all irrelevant extra contributions. We shall attempt to perform this cleaning in a statistical way.

3.2. The Galactic Mask

There are two alternatives to assess the Galactic contribution to the measured RM. The two ways differ by the population sample used for the assessment. If an independent population at the outskirts of the Galaxy exists, for which RM can be measured, this population can be used to map out the Galactic RM. We shall hereafter use the term "mask source population" for the set of objects by which we map the Galactic contribution to the RM.

An estimate for the thickness of the Galactic magnetic layer is ~ 1 kpc (Simard-Normandin & Kronberg 1980). That means that apart from the Galactic center direction, sources of distances that satisfy $r_{src} > 1/\sin(|b|)$ kpc (~ 3 kpc for $|b| = 20°$) are located beyond the Reynolds layer and fully probe the Galactic contribution to the RM. We hence consider two possibilities for the mask source population.

One natural candidate for this role is the pulsar population, for which RMs are available. In order to make use of the pulsars we need to find a subset of them that reside in the outer part of the Milky-way magnetic layer.
A class of pulsars that is especially appropriate for the task of probing the Galactic RM contribution is the millisecond pulsars. This population of old pulsars is believed to reside far out of the Galactic plane. The number density of millisecond pulsars as implied by a number of surveys at high Galactic latitude (~ 1 mJy sensitivity at ~ 1 GHz) ranges between $0.01 - 0.0175$ deg^{-2}, *i.e.* $400 - 700$ pulsars over the sky (Foster, Cadwell, Wolszczan, & Anderson 1995; Camilo, Nice, & Taylor 1996).

The alternative mask population for assessment of the Galactic RM contribution is a sub-set of the closest extragalactic sources. The disadvantage of using this population is the need for a large enough source number at low enough redshift, to allow differentiation between the cosmological contribution and the Galactic one. Exploiting extragalactic sources for the resolution of the Galactic contribution affects only slightly the amount of cosmological contribution correlation, as long as the nearby sources are taken within $z \lesssim 0.1$, since the bulk of the sources is at $z \gtrsim 1$ (*cf.* §4).

In order to use either one of the galactic mask populations, its number density should exceed a certain minimal number density. We now attempt to assess this minimal number.
The Galactic RM contribution is a two-dimensional field with RM values. The data on the other hand are made of distinctive sources located at discrete directions. The lines-of-sight to the Galactic mask population, do not necessarily coincide with the line-of-sight direction towards the extragalactic sources. The way to circumvent this difficulty is by introducing a *smoothed* version of the Galactic RM map, namely the field $\widehat{RM}_G(\hat{z})$. The two fields are connected via the smoothing angle θ_s, and by a specific choice of a Gaussian smoothing for N_G measurements of the Galactic $RM_G(\hat{z}_i)$ located at the directions $\hat{z}_i$

$$\widehat{RM}_G(\hat{z}) = \frac{\sum\limits_{i=1}^{N_G} RM_G^i \, \exp\left[-\frac{(\hat{z}_i - \hat{z})^2}{2\theta_s}\right]}{\sum\limits_{i=1}^{N_G} \exp\left[-\frac{(\hat{z}_i - \hat{z})^2}{2\theta_s^2}\right]} \ . \tag{22}$$

CEL. NORTH

CEL. SOUTH

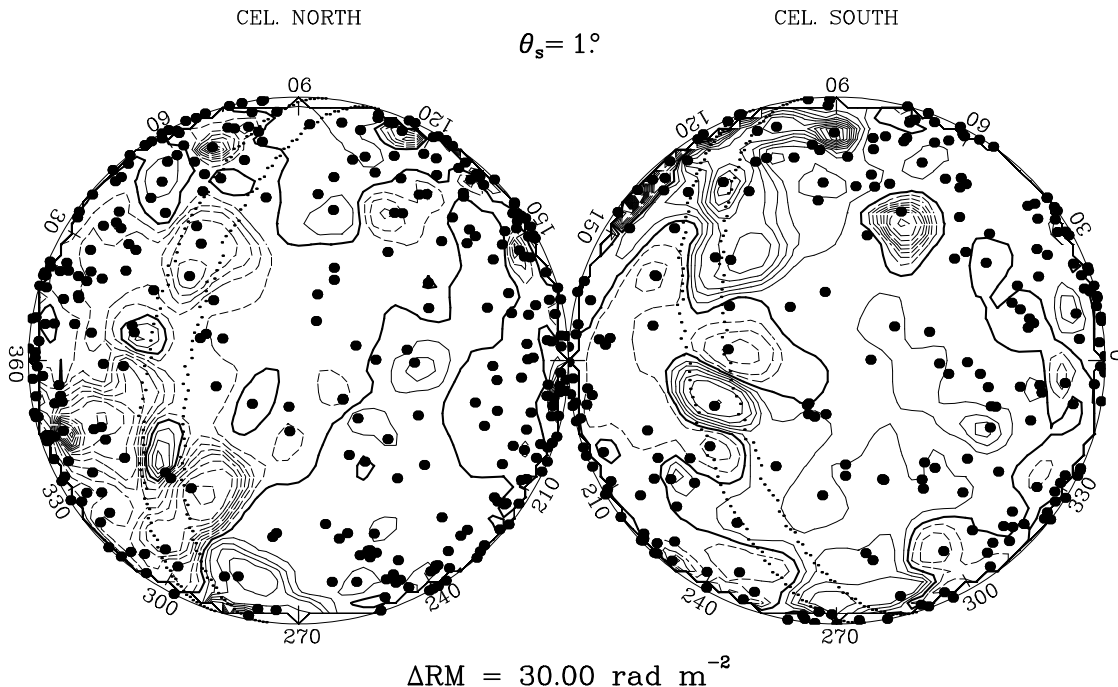$\theta_{\mathbf{s}} = 1°\!\!.$

ΔRM = 30.00 rad m^{-2}

Fig. 3.— The 1° smoothed RM Galactic mask projected onto celestial coordinates. Positive RM values marked by continuous lines and negative values by dashed lines. The RM = 0 line is thicker. The spacing is ΔRM = 30 rad m^{-2}. The locations of sources in the SKB catalog (projected) are marked by solid dots, and the Galactic plane is marked by the dotted strip.

When implemented using real data, the smoothing involves weights by measurement errors as well. For the purpose of this paper, we ignore these weights to avoid unnecessary complication. Using a smoothed field for the Galactic RM contribution, introduces random noise, ϵ_G, that can be directly evaluated by the very same N_G sample via

$$\epsilon_G^2 = \frac{1}{N_G} \sum_{i=1}^{n_G} \left(\mathrm{RM}_G(\hat{z}_i) - \widehat{\mathrm{RM}}_G(\hat{z}_i) \right)^2 . \tag{23}$$

The noise can be a function of position, it is difficult however to account for a position-dependent noise with low number of N_G. There are a few estimates in the literature for the noise level, ϵ_G, on different smoothing scales.

An upper limit for ϵ_G is given in Minter & Spangler (1996), who calculate the observed "structure function", D_{RM} which is the same as Eq. (23) but with an arbitrary lag γ and the unsmoothed values of the RM. They conclude that $D_{\mathrm{RM}}(\gamma > 1°) = (340 \pm 30)\gamma^{0.64\pm0.06}\mathrm{rad}^2\mathrm{m}^{-4}$, and drops steeper for $\gamma < 1°$. The value of the D_{RM} is an upper limit for $\epsilon_G^2(\gamma)$ as calculated here, due to the smoothing we apply (and was not applied in the D_{RM} calculation). Simonetti, Cordes, & Spangler (1984) calculate $D_{\mathrm{RM}} = 484 - 8100$ rad^{2}m^{-4}, depending on the Galactic latitude, for much larger
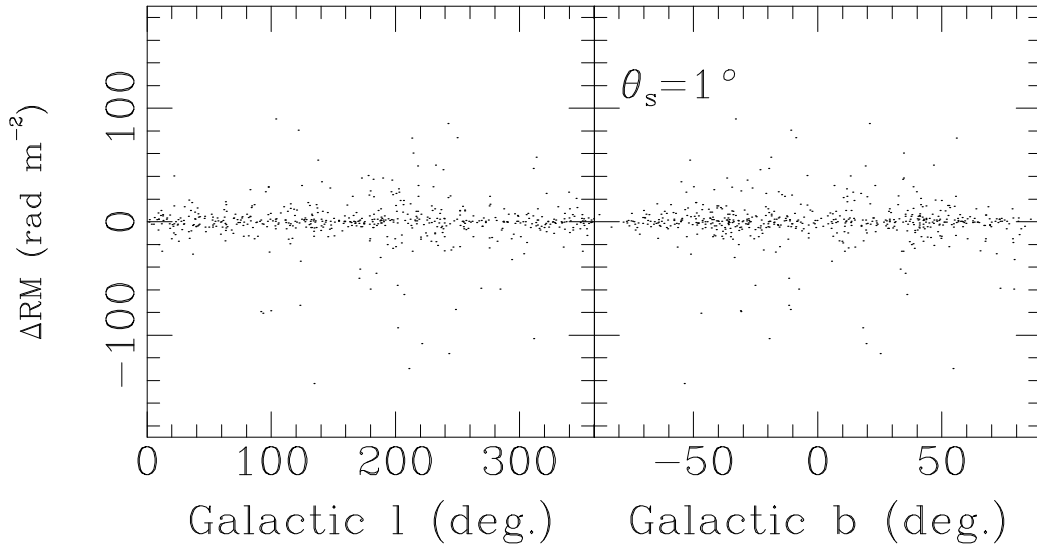
Fig. 4.— The RM residuals from the 1° smoothed Galactic mask as function of the Galactic longitude (left) and latitude (right).
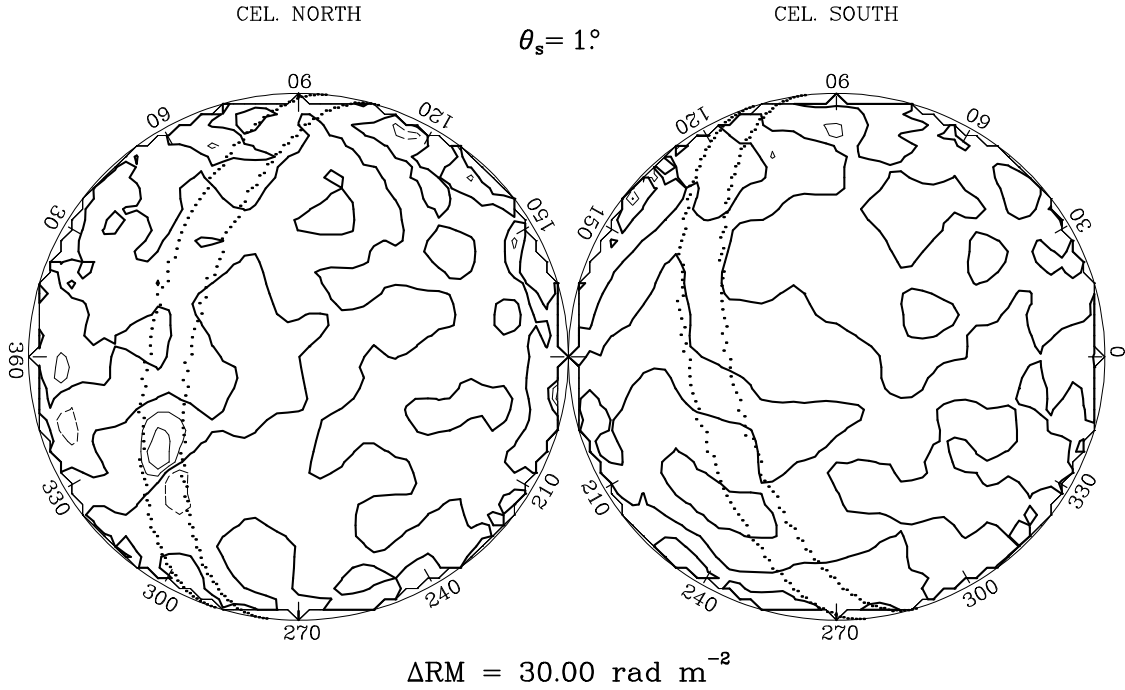

Fig. 5.— The 1° smoothed RM residuals of the Galactic mask in celestial coordinates. Symbols as in figure (3).

angular scales of $30° - 50°$! (linear scale).

Simonetti & Cordes (1986) corroborate these results and consider even larger angular scales to obtain typically $D_{RM} < 1000 \, \mathrm{rad^2 m^{-4}}$ on scales less than $100°$.

Oren & Wolfe (1995) calculate a very similar quantity to ϵ_G (with a varying top hat window instead of a fixed Gaussian), and obtain a typical variance of < 1000 rad^{2}m^{-4} on $\sim 30°$ scales.

All of these measurements suggest that for a mask population with number density of about one source per 1000 deg.^{2}, the Galactic contribution to the RM ($|b| > 20°$) can be resolved with a 1σ accuracy of 30 rad m^{-2}. That means that an isotropic coverage of about $100 - 200$ mask sources on the sky is enough for achieving this noise level.

"Damage control" for ignoring the position dependence can be devised by comparing the "clean" RM field dipole and quadrupole to the Galactic direction of the two. These first two multipole should be the most prominent signature of the Galactic RM mask.

We go back to the suggested mask populations and examine whether they are able to fulfill the requirement of the minimal number density.

The largest pulsar catalog to date [the electronic version of Taylor, Manchester, & Lyne (1993)] consists of 800 pulsars out of which 259 have RM measurements. This catalog was not compiled with a specific emphasis for millisecond pulsars, and therefore only 124 pulsars with RM values lie in Galactic latitude $|b| > 5°$. The softer condition $r_{src} > 2/\sin(|b|)$ (*i.e.* considering an "RM layer" of 4 kpc) is fulfilled for 237 pulsars with both RM registered value and estimated distance r_{src} (Taylor & Cordes 1993).

However, these 237 pulsars are still not distributed isotropically across the sky, and tend to concentrate near the Galactic plane.

A way to avoid this anisotropy is to compile a sample of millisecond pulsars, that lie far away from the Galactic plane. This population has a number density that exceeds the necessary $\sim 10^{-2}$ deg.$^{-2}$ by at least a factor of two and it may be as high as seven times denser than the minimal value. This population can be detected for RM (Fernando Camilo, private communication, 1997) [2] and ensures the $\epsilon_G \simeq 30$ rad m^{-2} noise level. This kind of sample is ideal for the current paper analysis, as it does not contain any cosmological contribution or internal RM contribution. The main disadvantage of it is that it does not exist yet.

In considering the extragalactic mask population; for the $\lesssim 400$ sources needed to resolve the Galactic contribution, it is sufficient to have a sample of 1mJy sensitivity (at a few GHz) up to $z \simeq 0.1$ [see Loan, Wall, & Lahav (1997) for the number density of radio sources with flux > 35 mJy, and Dunlop & Peacock (1990) for the combined flat/steep spectrum luminosity function for extrapolation to the 1mJy limit].

For this paper we follow Oren & Wolfe (1995) and use an extragalactic sample of RM measurements as an upper limit for the noise that appears by the Galactic RM removal procedure. The sample we use consists of 555 sources as listed by SKB. The SKB catalog allows us to realistically mimic the Galactic mask, and is an overestimate since we ascribe all the RM of the sources to the Galactic contribution. Moreover, unlike Oren & Wolfe we do not exclude "outliers". This use aims

---

[2]In the Taylor, Manchester, & Lyne catalog there are two pulsars with both RM registered value and $p < 10$ ms, and five for which $p < 100$ ms. The smallest polarized flux at 1.4 GHz for a pulsar with a registered RM is 0.2 mJy

to provide a realistic model of the Galactic mask contribution, and allows us to demonstrate the method power. For our purpose it should not be taken literally as the true Galactic mask contribution (even though Oren & Wolfe did consider it that way) because no segregation by redshift was applied to choose mask sources from the SKB list. We neither attempted to evaluate the internal RM (by means explained in §3.3) in order to minimize the ϵ_G value.

The SKB source locations (projected, and therefore concentrated toward the circumference) are marked as black dots on Figure 3 and shown on top of the smoothed Galactic RM field with smoothing scale of $\theta_s = 1°$. The smooth map is shown in celestial coordinates. Figure 4 shows the RM residuals as functions of Galactic latitude and longitude, and figure 5 shows the contour map of the smoothed residual field. Both figures (4 & 5) show hardly any longitude dependence of the residuals (in spite of the solar system off-center position), and bigger residuals in the $\sim \pm 20°$ strip about the Galactic plane (*cf.* the same conclusion of Oren & Wolfe 1995). In an all-sky coverage of sources, this residual deviation should be of some worry, but as we shall see (§4.2), it doesn't bias the result for the most likely power spectrum as calculated by the Bayesian analysis. If the analysis is confined to high latitudes, then no systematic error due to the Galactic mask is expected (*cf.* §4). For a few square degrees area, we notice there are typically no significant gradients in the Galactic RM field beyond $|b| \gtrsim 30°$. This allows us to use the smooth value safely when analyzing a small area with extragalactic RM measurements. This value is also consistent with all the abovementioned values of D_{RM} as obtained by more detailed analyses.

3.3. The Internal Variation and foreground screens

We would like to get an estimate for the internal RM contribution and for the foreground screen contribution (if the latter exists). We do not attempt to correct each individual source for the RM contribution due to the internal and foreground screen terms. We *do not* take the measured RM and subtract an estimate for RM_{I+f}, we rather attempt to estimate the distribution of RM_{I+f}, and treat it as another noise term.

The difference between the two separate terms in Eq. (21) (RM_I and RM_f) emerges from the fact that while the internal contribution is obtained from the same medium that emits the polarized light, the foreground screen only serves as a filter for an already existing signal. In previous investigations, attempts were made to separate the two contributions (Burn 1966; Laing 1984), later on it became clear that the signature of the two is rather similar (Tribble 1991).

For our purposes we are interested in all previous calculations' "left overs", their signal is our noise and vice versa. For the noise estimate we claim it is legitimate to take the internal contribution and the foreground screen contribution together. We argue that the two can be dealt with simultaneously. To this end we shall use the other piece of information provided by the observations – the polarization degree.

Tribble (1991) shows the connection between the observed depolarization (as a function of

wavelength) and the observed RM for an extended source. Using this connection, and provided the polarization measurements are available, a direct estimate for the internal RM can be carried out. Recall we do not expect any depolarization due to the cosmological RM since the cosmological coherence we are after is orders of magnitude bigger ($\gtrsim$ a few h^{-1}Mpc) than the source size.

It is interesting to note, that even if we had perfect information about the depolarization due to the source structure and foreground screen contribution and an exact relation between the depolarization degree and the RM, we could still not subtract this derived RM from the observed one. This is due to the fact that the polarization degree doesn't specify the RM direction.

Tribble's statistical connection between the observed depolarization and the observed RM is valid only if the correlation scale of the RM structure function for the source or the foreground screen is much shorter than the telescope beam size. This condition is probably not valid for individual damped Lyman–α systems, and galaxies that serve as foreground screens, and for which long range correlation across the telescope beam may exist.

Full justification for neglecting damped Lyman–α systems and galaxies exists only if we can avoid lines-of-sight that cross such systems. Otherwise the order of magnitude of an intervening galaxy contribution is obtained as follows: For a galaxy seen face-on, where there is a danger of a well ordered magnetic field, the disc thickness, to which the magnetic field is presumably connected is of the order of kpc (Simard-Normandin & Kronberg 1980). Observations show magnetic field magnitude of $\sim \mu$G, mainly in the disc plane. In order to equate this to a cosmological magnetic field of the order of nG, and coherent scale of 50 h^{-1}Mpc, the average baryon number density across the galaxy should be at least fifty times higher than the cosmological $\bar{n}_b$.

However, we do not expect any correlation between the magnetic field orientation of galaxies along the line-of-sight, or galaxies adjacent (in angle) to each other. The worst contribution to the RM, could only come from a random walk of N_f steps where N_f is the number of foreground screens (intervening systems) along the line-of-sight. Since one can model the probability for an intersecting system along the line-of-sight as a function of the source redshift (Welter, Perry, & Kronberg 1984; Lanzetta, Wolfe, & Turnshek 1995), another noise term can be added. We did not attempt to model this noise term here, because we believe that the best strategy would be to avoid highly contributing (*i.e.* damped Lyman-α and Lyman limit) intervening systems. Low column density Lyman-α system contribute very little to the RM signal (see Eq. (1.2) in Welter, Perry, & Kronberg 1984). An exception may exist, if two sources (or two separated parts of the same source) cross the same cluster. In that case the noise of the two sources (RM_{I+f}) may be correlated, but then we can go back to the technique that uses the depolarization, in an attempt to remove the noise correlation.

The best strategy, as stated earlier, would be to avoid intervening systems altogether. There are two methods for doing this. The first method is simply to avoid intervening systems by looking for sources that exhibit no absorption lines in their spectra (we assume spectrography is carried out anyway, to allow redshift determination). The existence of a large fraction of quasar lines-of-sight which do not intersect a dense intervenor is corroborated by Møller & Jakobsen (1990) and

Lanzetta, Wolfe, & Turnshek (1995) analyses.

The other method is to put a depolarization limit on the observations (*e.g.* the one imposed by Tabara & Inoue 1979). Such a limit naturally reduces the noise term of ϵ_{I+f} and does not affect the correlation signal. As a matter of fact, a sequence of such depolarization limits, may be helpful in constituting the estimate for ϵ_{I+f}. There are yet more methods for minimizing the number of sources that manifest internal RM as we shall point out when we consider real observations (§5).

3.4. Bayesian Likelihood Analysis

In the current stage of research we have very little knowledge about the power spectrum of the cosmological magnetic field. We can hardly even put limits on its integral value, *i.e.* the rms value of the field. There are, however predictions regarding the power spectrum shape and amplitude. In the lack of any observational preference towards any of these predictions (apart from the limits on its rms value), we assume that all models are equally probable. Conventional estimates of the RM correlation, estimates of the sort applied to galaxies are not very useful. It is difficult to get correct error estimate without simulations, that in turn must assume some magnetic field power spectrum, moreover in the traditional correlation calculation procedure, the errors of different bins in r space are correlated. On top of that, the quantity we are after is the magnetic field power spectrum, and the inversion from the integrated RM back to the magnetic field is a non-trivial one. All of the above lead us to the use of Bayesian statistics as a tool for finding the best parameters, and their probability, given a model. In the Bayesian formalism, the a-posteriori probability density of a model, $\mathbf{m}$, given the data, $\mathbf{d}$, is

$$\mathcal{P}(\mathbf{m}|\mathbf{d}) = \frac{\mathcal{P}(\mathbf{m})\mathcal{P}(\mathbf{d}|\mathbf{m})}{\mathcal{P}(\mathbf{d})} \, . \tag{24}$$

As stated earlier, $\mathcal{P}(\mathbf{m})$, the model probability density is unknown and therefore assumed uniform for all models. The data probability, in the denominator is the same for all models, and therefore serves as a normalization factor. We are thus left with equivalence between the operation of maximizing the probability of the model, given the data $[\mathcal{P}(\mathbf{m}|\mathbf{d})]$ and the operation of maximizing the probability of the data, given the model $[\mathcal{P}(\mathbf{d}|\mathbf{m})]$. This equivalence allows us to write down the likelihood function for N_{src} sources with measured RM.

We begin by constructing the $N_{src} \times N_{src}$ symmetric matrix Υ_{ij} of the expectation values for the RM correlation (Eq. 15) between these sources (as determined by their position). We further assume that the errors in each RM value are uncorrelated and Gaussianly distributed. The variance of the overall error is the sum of the quadratures of the various error sources *i.e.*

$$\epsilon_i^2 = \epsilon_G^2 + \epsilon_{I+f,i}^2 + \epsilon_{m,i}^2 \, , \tag{25}$$

and the likelihood function becomes

$$\mathcal{L} = [(2\pi)^{N_{src}} \det(\tilde{\Upsilon}_{ij})]^{-1/2} \exp\left(-\frac{1}{2} \sum_{i,j}^{N_{src}} \mathrm{RM}_i \tilde{\Upsilon}_{ij}^{-1} \mathrm{RM}_j \right) \, , \tag{26}$$

where $\tilde{\Upsilon}_{ij} = \Upsilon_{ij} + \delta_{ij}^K \epsilon_i^2$.

The χ^2 statistic is defined as $\chi^2 = -2\ln\mathcal{L}$. The χ^2 statistics as defined, is a χ^2 distribution (of N_{src} degrees of freedom) with respect to the *data points*, not the model parameters. This χ^2 is interpreted as a rough estimate for the confidence levels in the *parameter* space.

3.5. Estimating the Signal-to-Noise Ratio

Before proceeding to the elaborated description of the various tests we performed with artificial data, we would like to get a rough estimate for the expected RM correlation and the necessary number of sources for a high enough signal-to-noise ratio at various scales. We temporarily abandon the Bayesian approach, and focus on $\mathcal{P}(\mathbf{m}|\mathbf{d})$. Recall that the noise in the cross correlation is not correlated, but may still dominate the signal if not appropriately averaged over many pairs. The signal-to-noise ratio for an individual measurement of a pair at identical redshift, a separation angle γ, and in the context of a specific model, is given by

$$\left\langle \frac{\Upsilon(z,\gamma)}{\epsilon^2} \right\rangle = \frac{\langle \Upsilon(z,\gamma) \rangle}{\langle \epsilon^2 \rangle} , \qquad (27)$$

where in the last equality we assume no dependence between the various noise terms and the model (cosmology + power spectrum). The cosmological parameters we choose to use are as follows: We restrict ourselves to flat cosmology with $\Omega_m = 1$, we choose $H_0 = 100$ km s^{-1} Mpc^{-1} (but the scaling with h is straightforward). We take the ionization factor to be $X_n = 1$ which according to the Gunn-Peterson effect (Gunn & Peterson 1965) is a reasonable choice, and $\Omega_b = 0.024h^{-2}$ (Tytler, Fan, & Burles 1996), *i.e.* $\bar{n}_b = 2.6 \times 10^{-7}$ cm^{-3}.

For N_{pair} pairs where each source is a member of one pair only, the signal-to-noise can further be increased by $\sqrt{N_{pair}}$. In figure 6 we plot the necessary number of pairs in order to achieve a signal to noise ratio of $Q = 3$. All sources are assumed to be at the same redshift (2, 1, or 0.5), we take the noise values $\epsilon_G = 32$ rad m^{-2} (this is the value for $\theta_s = 1°$). For the noise term due to the internal RM and the (possible) foreground screen we use the Tabara & Inoue (1979) catalog as a guideline. Tabara & Inoue listed ~ 1500 radio sources in their catalog with RM $\lesssim 200$ rad m^{-2}. That means a $\sim 3.4\sigma$ cover, and gives $\sigma_{RM,obs} \simeq 59$ rad m^{-2}. The most conservative assumption one can make is to attribute all of this RM to the internal and foreground screen contribution. The procedure for deriving the internal and foreground screen contribution from the depolarization (*cf.* § 3.3) bears noise itself and is correct only statistically. We model its accuracy as a Gaussian with one quarter the width of the observed RM distribution. Doing so we end up with $\epsilon_{I+f} = (59^2 + 15^2)^{1/2} \simeq 61$ rad m^{-2}. This is a conservative choice, and the true value for ϵ_{I+f} is probably much smaller. Note for instance the $\epsilon_{I+f} \simeq 20$ rad m^{-2} value as obtained by Oren & Wolfe (1995). The measurement errors are neglected (*cf.* § 3.1). Two power spectra are considered and they are both normalized to give $B_{rms}^{TH}(50 \text{ h}^{-1}\text{Mpc}) = 1$ nG (the $n = 0$ case gives results between the $n = -1$ and the $n = 1$ power spectra). A typical number of pairs for achieving a signal to noise ratio of ~ 3 in the range $\gamma \lesssim 0.5$ is between 10 and 2×10^3 pairs, depending on the power spectrum.
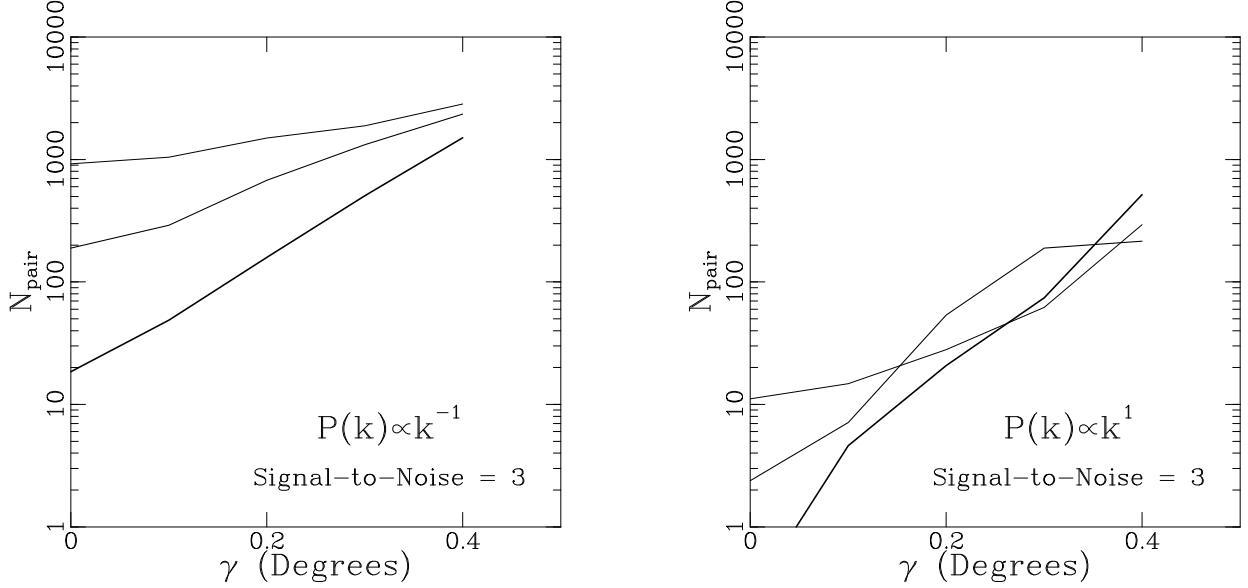
Fig. 6.— Estimate of the number of pairs at separation γ needed to achieve signal to noise ratio of 3. The magnetic field is normalized by $B_{rms}^{TH}(50\ \mathrm{h}^{-1}\mathrm{Mpc}) = 1$ nG, and the noise calculation is explained in the text. Two cases for power index of -1 (left) and 1 (right) are plotted.

This estimate of Q is not accurate. To begin with, for N_{src} sources we expect less than $(N_{src}^2 - N_{src})/2$ statistically independent pairs. We do not expect all sources to reside at the same redshift, neither do we expect the errors to be identical for all sources. Furthermore, the separation between the sources is not fixed , but rather is spread from the arc-minute scale to $180°$. Due to the need for a realistic error estimate, and a demonstration of an actual implementation of the technique we propose, led us to apply it to mock catalogs, for which the underlying power spectrum is known.

4.   TESTING WITH ARTIFICIAL DATA

As a reliable probe for our method we create artificial catalogs of radio sources for which RM values are measured. We first generate a Gaussian random field of the magnetic vector potential, $\vec{A}$ with the power spectrum $P_A(k) = k^2 P_B(k)(= E(k))$. The realization takes place on a 256^3 grid points equally spaced in comoving coordinates. The $P_B(k)$ power spectrum is Gaussianly smoothed on the one grid cell scale. The amplitude of the field is arbitrary. We then derive the magnetic field itself by the real space relation $\vec{B} = \vec{\nabla} \times \vec{A}$ translated to k space *i.e.* $\vec{B}(\vec{k}) = -i\vec{k} \times \vec{A}$. We use the k space symmetries due to the real nature of the $\vec{A}$ field (no imaginary part), and go back to real

space to obtain a divergence-free magnetic field with the desired correlation function, and periodic boundary conditions. We check the resultant field by calculating the field divergence about each and every grid point in real space and get $\vec{\nabla} \cdot \vec{B}/B_{rms} < 5 \times 10^{-5}$.

At this point we select the cosmology into which we embed the simulation. Our standard choice is identical to the one described in the signal-to-noise estimate (§ 3.5). Due to the limited dynamical range, we choose the grid scale to represent 1.5 h^{-1}Mpc, and we are therefore confined to a largest simulation wavelength of 768 h^{-1}Mpc.

We then select the source mask, *i.e.* the source distribution across the sky, and their redshifts. The two-dimensional distribution is taken to be a Poisson-like distribution, this choice allows us to have close pairs (unlike grid selection), but to be as conservative as possible in terms of the angular correlation function of the sources. Introducing any correlation as observed for radio sources (Kooiman, Burne & Klypin 1995; Sicotte 1995; Cress *et al.* 1995; Loan, Wall, & Lahav 1997) can only increase the number of close pairs on small angles, and thus improve the RM correlation resultant signal (see fig. 6). We do not take explicitly into account very small angle (sub arc-minute) separations that may exist in real data sets for resolved extended sources, whose different parts can be used as more than one background source. We employ two distribution schemes, an all-sky coverage, and a cover of 150 deg.^{2} area centered about the north Galactic pole.

The source redshift distribution is selected according to the $N(z)$ of radio sources with flux > 35 mJy (at 4.85 GHz) as calculated by Loan, Wall, & Lahav (1997) who used the mean of the theoretical luminosity function models of Dunlop & Peacock (1990) and kindly provided their fit. Loan *et al.* (1997) $N(z)$ is peaked around $z = 1$, and has a shape resembling a low redshift truncated Gaussian of width $(2 \times \sigma)$ $\Delta z \simeq 1.9$.

In principle, setting flux limit and sky coverage, sets the source number. In practice only a sub-set of all radio sources emit polarized light. A random sample taken from the NVSS survey (Condon *et al.* 1994) shows registered polarization angle for $\sim 40\%$ of the sources. Refraining from sources with intervening systems and large internal RM may further decrease the number. Since the source number density in the radio catalogs of this flux limit is a few per square degree, when we prepare an "all-sky" coverage catalog (see below), we are always way below the available number of sources. For smaller angular coverage with higher source density, one has to further decrease the flux limit. For example in the 2.5 mJy limit we expect ~ 50 sources per square degree (NVSS, Condon *et al.* 1994), and in the 1 mJy limit we expect source density of about 100 per square degree (the "FIRST" survey; Becker, White, & Helfand 1995).

The $N(z)$ function of Loan *et al.* (1997) is therefore interpreted as a normalized selection function, with a cutoff at the highest redshift of the catalog. We expect this selection function to provide an underestimate for the number of sources at high redshift, if a lower flux limit is set. Since sources at higher redshift typically bear higher signal (without changing the noise), such an imposed selection is a conservative choice in terms of the expected signal-to-noise ratio [3].

---

[3]The $N(z)$ we choose, which is peaked in a relatively low redshift, may be useful in mimicking another effect. As

For each selected source, we integrate along the line-of-sight over the dot product between the magnetic field and the line-of-sight direction using the periodic boundary conditions. The integration scheme assigns weights to each integration segment, k, according to

$$w_k^B = \frac{(1 + z_k)^3}{\sqrt{1 - K r_k^2(z_k)}} \,, \tag{28}$$

in order to account for the cosmological evolution.

We then add the following noise terms to the resultant RM

1. Internal variation + foreground screens.

   We draw this noise term from a Gaussian of $(59\,\mathrm{rad\,m^{-2}})^2$ variance (*cf.* § 3.5). This is the added RM to the cosmological one. However, we also try to imitate the procedure of ϵ_{I+f} evaluation by the depolarization. To this end, for a specific value of RM_{I+f}^i (drawn earlier), we mimic the recovery of the ϵ_{I+f} from the depolarization degree, by listing an ϵ_{I+f} value scattered about RM_{I+f}^i. The scatter has a Gaussian distribution of $(15\,\mathrm{rad\,m^{-2}})^2$ variance. This is the error in the noise estimate. The "observer" takes into account the scattered value of the ϵ_{I+f} and not the value that was actually added to the integrated cosmological RM.

2. Galactic mask.

   We use the model-estimate of the Galactic mask, smoothed to $1°$ scale (see § 3.2). Since the smoothed galactic RM differs from the true RM to the line-of-sight, we add a RM drawn from a Gaussian distribution with the standard deviation of $\epsilon_G = 32\,\mathrm{rad\,m^{-2}}$ (Eq. 23).

At the end of this process we are left with a mock RM catalog that consists of source coordinates and redshift, measured RM value, and the total error in the RM value (*i.e.* ϵ_{I+f}).

We proceed by feeding the mock catalog into the maximum likelihood procedure. In the current application, we consider only the right cosmology, *i.e.* the one in which the simulation was embedded. In principle the sensitivity to the cosmology choice can be checked as well. The two variables for the model are the amplitude and the power index. It is really the combination of the two that the likelihood procedure constraints best.
The statistical significance of the χ^2 distribution (as defined following Eq. (26)) is obtained in the standard way. The number of degrees of freedom is the source number minus the number of fitting parameters, and the goodness of fit is calculated by taking into account the value of χ^2_{min}. If the goodness of fit turns out to be very small (< 0.1), this is a clear indication for convergence to the wrong minimum, and vice versa. For the right solution the minimum value for the χ^2 per degree of freedom (the source number) is typically unity within 10^{-3} accuracy.

the source redshift increases, the probability for intervening systems along the line-of-sight increases as well. If in a sample compilation we try to avoid intervening system, this attempt translates to a steeper fall-off of the selection function.

4.1.   Partial Sky Coverage

We first explore partial sky coverage mock RM catalogs. Figures 7 show contour maps of $\chi^2 - \chi^2_{min}$ with steps of unity. The thicker lines indicate the approximate $1, 2$, and 3σ levels of the probability function as ascribed by using two parameter χ^2 statistics (*cf.* §3.4). The power spectrum normalization is our standard $B^{TH}_{rms}(50 \text{ h}^{-1}\text{Mpc}) = 1 - 5$ nG, depending on the power spectrum. We use $500-800$ sources for the part sky and 150 square degrees coverage. The different source number and B_{rms} values reflect the fact that we have fixed the angular sky coverage. That in turn translates differently for different spectra. A redshift cutoff of $z < 5$ has been applied. Figure 8 shows a particular example for the case $n = 1$, where we have increased $B^{TH}_{rms}(50 \text{ h}^{-1}\text{Mpc})$ to the 17 nG level in order to verify the result dependence on B_{rms}.

We notice that for all power spectra, the Bayesian approach recovers the correct value from the artificial catalog (marked by a cross sign) to within the 1σ level. The method is more robust with respect to the amplitude determination. The power index is not well bound unless it is very different from the true one. The method (with the limited number of sources) tends to recover best the B_{rms} value on a certain scale, which is a combination of the power index and the amplitude. Typical values for the ratio between the true B_{rms} and the minimization result for B_{rms} are in the range $0.6 - 1.5$.

Partial sky coverage is preferable in terms of the number of small separation pairs, and the indifference to the Galactic mask variation as function of direction. A collection of several of these small patches is expected to provide an even better constrain on the magnetic field power spectrum, but the analysis becomes a bit more complicated, as one should also include the large scale correlation between the patches without increasing the noise from the auto correlation to an intolerable level.

Given the relatively big errors, we desire off-diagonal terms in the correlation matrix to be as big as possible (*i.e.* small separation). This is meant to avoid heavy weight for diagonal terms which are dominated by noise. The price for choosing small patches with small sky coverage is limited ability to constrain the power index. Under special conditions, this ability can be partially recovered by turning to an all sky coverage as we discuss in the next section.

4.2.   All Sky Coverage

An all sky coverage, with the small correlation scales that are tested here, is impractical without lowering the error level significantly. Otherwise the Bayesian analysis will all be dominated by the diagonal terms with a large noise added to them and one loses the advantage of the correlation scheme for noise reduction.

All sky coverage is however still feasible if we design the sample very carefully. In order to minimize the Galactic noise we should observe sources in proximity to the mask sources direction and avoid the necessity for smoothing the Galactic mask. Instead, the RM values as deduced
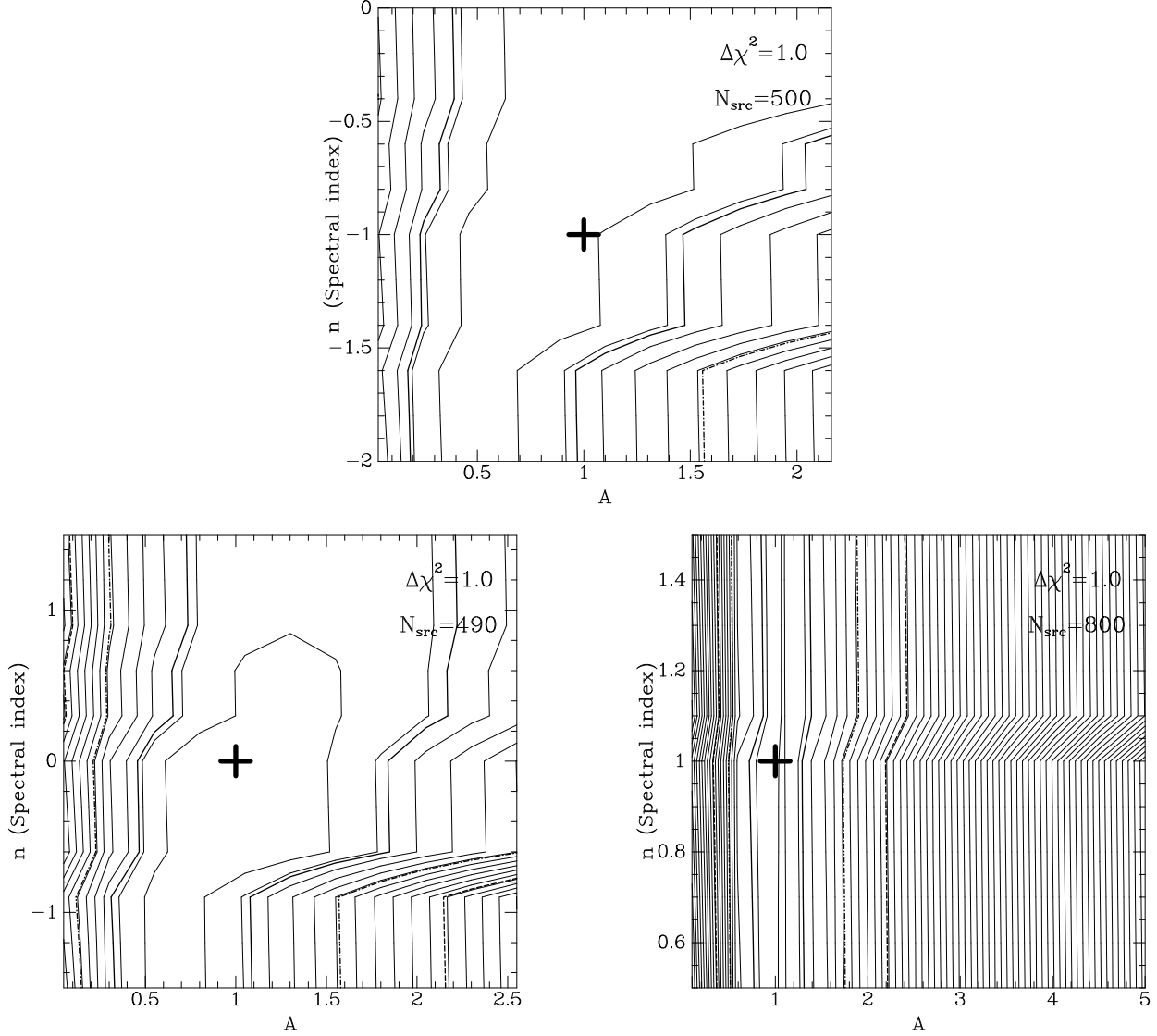
Fig. 7.— Contour plot of $\chi^2 - \chi^2_{min}$ (as defined following Eq. (26)) in the amplitude - spectral index plane. The amplitude is in units of the true simulation amplitude. The spacing is of $\Delta\chi^2 = 1$, and confidence levels for $1, 2,$ and 3σ are plotted (bold lines) as if the contours obey χ^2 statistics in the two-dimensional parameter space. The true value of the simulation is marked by the cross sign. All plots are for a part sky coverage of 150 deg.^{2} about the Galactic north pole. The values for $B^{TH}_{rms}(50 \ h^{-1}Mpc)$ are 5, 2, and 1 for $n = -1,$ 0, and 1 (top, left, right) respectively. The total number of sources is marked on the plots.

from the mask source population can simply be subtracted from the observed RM values. The small variation in the Galactic magnetic field on small scales (Simonetti, Cordes, & Spangler 1984; Simonetti & Cordes 1986; Minter & Spangler 1996) allows this subtraction to take place.

If on top of that one can reduce the noise from internal RM to the level of 5 rad m^{-2} (one

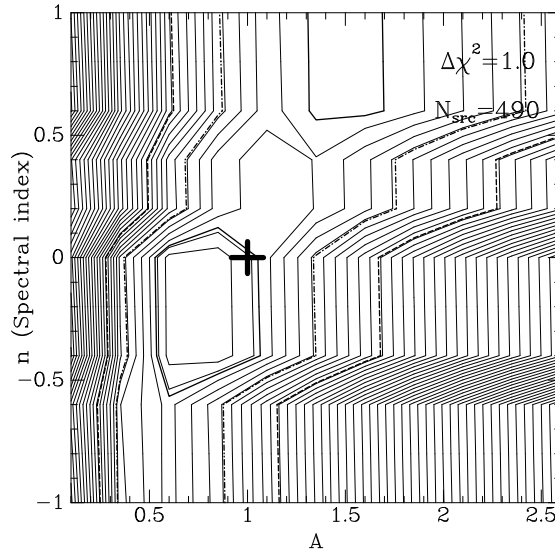Fig. 8.— Same as the $n = 0$ panel in the previous figure (fig. 7). Here $B_{rms}^{TH}(50 \ h^{-1}\text{Mpc})$ is 17 nG, and allows a better determination of the parameters.

can always avoid foreground screens) by multi wavelength observations, then it becomes sensible to exploit an all-sky coverage.

Figure 9 shows an example of a sample taken at the mask source directions with $\epsilon_I = 5 \ \text{rad m}^{-2}$ and $B_{rms}^{TH}(50 \ h^{-1}\text{Mpc}) = 1$ nG. The rest of the parameters are identical to those of the part sky coverage ($n = 1$) of the last section. We notice that the power index is somewhat better constrained in an all sky coverage, especially if the amplitude (or B_{rms}) are assumed or known from some different source. The true values are recovered to within the $\sim 2\sigma$ level. Moreover such coverage allows us to calculate all prevailing magnetic fields on the sample scale, expressed as $P_B(k) = \delta^D(k - \frac{\pi}{R})$ with δ^D the Dirac delta function and R the sample depth. Notice, however that using the formalism proposed in section 2, we cannot take into account power spectra that are not functions of $|k|$ alone so this test is a bit weaker than the dipole test.

5. DISCUSSION AND CONCLUSIONS

We have presented the formalism for the RM correlation function and demonstrated that by using it we can put limits on the power spectrum of the cosmological magnetic field. These limits are more stringent than limits obtained by any other method that currently exists. Limits of $2 - 3\sigma$ level for magnetic field of ~ 1 nG on inter-cluster scales ($\sim 50 \ h^{-1}\text{Mpc}$) can be devised with only $10^2 - 10^3$ sources. The increment of the source number reflects linearly in the B_{rms} limits.

We performed the statistical analysis following a Bayesian approach that seems to be the most adequate for this problem. The correlation method we propose is also less susceptible to systematic effects such as observational bias (or bias due to evolution) toward smaller internal RM measures
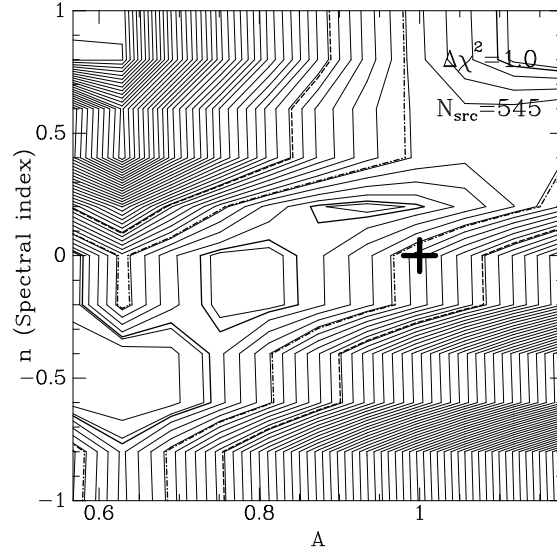
Fig. 9.— Contour plot of $\chi^2 - \chi^2_{min}$ in the amplitude - spectral index plane (same as figure (7)) for an all-sky coverage of sources in the mask sources directions. The internal scatter in RM is assumed to be considerably lower than in the part sky coverage and $B^{TH}_{rms}(50\ h^{-1}\mathrm{Mpc}) = 1$ nG.

for higher redshift sources. Both of these biases tend to lower the expected correlation signal as the source redshifts increase, whereas a cosmological magnetic field tends to raise the correlation signal between such sources.

In order to estimate the statistical significance of limits as derived by the proposed method, we have simulated a few possible cosmological magnetic fields. The simulations allow us to have a fair estimate of the errors involved in the power spectrum derivation. The analysis depends, however on a few assumptions, and most crucially on the ability to eliminate or estimate the foreground screen and internal contribution to the observed RM.

This crucial point can be addressed in the process of the sample compilation. Reduction of the foreground screen and internal RM contribution is achievable by applying two cutoff criteria to the sample. The first cutoff in minimal polarization degree is meant to avoid sources that exhibit large depolarization degree. These sources are usually interpreted as having a big non-cosmological contribution to their measured RM. The second cutoff is for sources that do not follow a λ^2 dependence of the RM. Following Laing's (1984) recipe, in order to minimize the number of sources with internal RM, the wavelength span should allow detection of deviation from the λ^2 dependence of the RM for $\phi > \pi/2$. Should this deviation occur, the source is to be eliminated from the catalog as a suspect for substantial internal RM contribution.

On top of the abovementioned cutoffs, all sources should preferably be detected for absorption lines, as a method to eliminate sources with intervening systems along the line-of-sight to the sources.

The spatial coverage of the sky should be twofold. Small patches of a few square degrees

enable the small separation pair number needed for noise reduction. Small patches, however, can not reveal large correlation scales in an effective way. It is thus desirable to compile a dilute all sky coverage sample, in addition to the high number density patches off the Galactic plane. The two sampling strategies cover a large range of potential correlation scales, without the necessity for an all-sky dense sample. The all sky coverage should preferably look for sources in proximity to the mask sources directions in order to minimize the Galactic noise term. Accurate internal RM for these sources should be evaluated through depolarization measurements in order for them to be useful for the power spectrum evaluation. Ultimately, the sample can always be mimicked in terms of the exact source locations in the framework of all and every detected model. Exact imitation of the source locations ensures the right correlation terms in the correlation matrix.

The limits we have derived here are a combination of limits on the free electron average density, $\bar{n}_e$, and the magnetic field. If by any other fashion (like HII absorption) an estimate for $\bar{n}_e$ can be achieved, then the limits on B will become more robust. The estimate is also a function of the assumed cosmology, and may be entangled with magnetic field evolution in the post recombination era. We haven't modeled such evolution in this paper.

This method of RM correlation can further be generalized to the *smoothed* RM correlation. The data can be smoothed on a certain angular scale, and then either compared to the expectation value predicted by a model, or inverted numerically to give limits on B. The Bayesian approach, though ceases to be advantageous in the smoothed case, because even though the noise terms decrease, the smoothing introduces correlation among the errors, and the statistical interpretation becomes more hazardous.

A nice feature of the proposed analysis is that it is bound to yield results. These can be either limits on the magnetic field magnitude, or actual detection of its value. Either way, these results may help in lifting the curtain over the mystery of the cluster and galactic magnetic fields origin.

REFERENCES

Adams, J., Danielsson, U.H., Grasso, D., & Rubinstein, H. 1996, sissa preprint, astro-ph/9607043

Barrow, J.D., Ferreira, P.G., & Silk, J. 1997, sissa preprint, astro-ph/9701063

Baugh, C.M. 1995, sissa preprint, astro-ph/9512011

Baugh, C.M. and Efstathiou, G. 1993, MNRAS, 265, 145

Becker, R.H., White, R.L., & Helfand, D.J. 1995, ApJ, 450, 559

Boyle, B.J. 1986, PhD thesis, University of Durham

Brandenburg, A., Enquist, K., & Olesen, P. 1996, sissa preprint, asrto-ph/9602031

Broten, N.W., Macleod, J.M., & Vallée, J,P. 1988, Ap&SS, 141, 303

Burn, B.J. 1966, MNRAS, 133, 67

Camilo, F., Nice, D.J., & Taylor J.H. 1996, ApJ, 461, 812

Cheng, B.L., Olinto, A.V., Schramm, D.N., & Truran, J.W 1996, Phys. Rev. D, 54, 4714

Condon, J.J., Cotton, W.D., Greisen, E.W., Yin, Q.F., Perley, R.A., & Broderick, J.J. 1994, in
    Astronomical Data Analysis Software and Systems III, A.S.P. Conference Series, Vol. 61
    Eds. Dennis, R. Crabtree, R.J., Barnes H., & Barnes, J. p. 155

Cress, C.M., Helfand, D.J., Becker, R.H., Gregg, M.D., White, R.L. 1996, ApJ, 473, 7

Dolgov, A. & Silk, J. 1993 Phys. Rev. D, 47, 3144

Dunlop, J.S. & Peacock, J.A. 1990 MNRAS, 247, 19

Foster, R.S., Cadwell, B.J., Wolszczan, A., & Anderson, S.B. 1995, ApJ, 454, 826

Grasso, D. & Rubinstein H.R. 1995, Nucl. Phys. B, 43, 303

Grasso, D. & Rubinstein H.R. 1996, Phys. Let. B, 388, 253

Gunn, J.E. & Peterson, B.,A. 1965, ApJ, 142, 1633

Harrison, E.R. 1973, Phys. Rev. Lett., 30, 18

Kato, T., Tabara, H., Inoue, M., & Aizu, K. 1987, Nature, 329, 223

Kolb, E.W. & Turner, M.S. 1990, *The Early Universe*, (USA: Addison-Wesley) p. 84

Kooiman, B.L., Burns, J.O., & Klypin, A.A. 1995, ApJ, 448, 500

Kronberg, P.P. 1976, *Int. Astron. Union Symp.* 74, 367

Kronberg, P.P. 1994, Rep. Prog. Phys., 57, 325 (K94)

Kronberg, P.P. & Simard-Normandin, M. 1976, Nature, 263, 653

Laing, R.A. 1984, in *Physics of Energy Transport in Extragalactic Radio Sources*, edited by Bridle,
    A.H. & Eilek, J.A. (Green Bank W.Va. USA:NRAO) p. 90

Lang, K.R. 1978, *Astrophysical Formulae*, (New-York: Springer-Verlag) p. 57

Lanzetta, K.M., Wolfe, A.M., Turnshek, D.A. 1995, ApJ, 440, 425

Lee, S., Olinto, A.V., & Sigl, G. 1995, ApJ, 455, L21

Loan, A.J., Wall, J.V., & Lahav, O. 1997, MNRAS, 286, 994

Loeb, A. & Kosowsky, A. 1996, ApJ, 469, 1

Masden, M.S. 1989, MNRAS, 237, 109

Minter, A.H. & Spangler, S.R. 1996, ApJ, 458, 194

Møller, P. & Jakobsen, P. 1990, A&A228, 299

Monin, A.S. & Yaglom, A.M. 1975, *Statistical Fluid Mechanics* (Cambridge; MIT Press), pp. 29–52

Nissen, D. & Thielheim, K.O. 1975, Ap&SS, 33, 441

Oren, A.L. & Wolfe, A.M. 1995 ApJ, 445, 624

Osmer, P.S. 1981, ApJ, 247, 762

Ostriker, J.P. & Thompson, C. 1987, ApJ, 323, L97

Parker, E.N. 1979, *Cosmical Magnetic Fields* (Oxford; Clarendon Press) p. 616

Pudritz, R.E. & Silk, J. 1989, ApJ, 342, 650

Quashnock, J.M., Loeb, A., & Spergel, D.N. 1989, ApJ, 342, 650

Ratra, B. 1992a, Phys. Rev. D, 45, 1913

Ratra, B. 1992b, ApJ, 391, L1

Rees, M.,J. 1987, QJRAS, 28, 197

Sicotte, H., 1995, Ph.D. thesis, Princeton University

Simard-Normandin, M. & Kronberg, P.P. 1980, ApJ, 242, 74

Simard-Normandin, M. & Kronberg, P.P., & Button, S. 1980, ApJS, 45, 97 (SKB)

Simonetti, J.H., Cordes, J.M., & Spangler, S.R. 1984 ApJ, 284, 126

Simonetti, J.H. & Cordes, J.M. 1986 ApJ, 310, 160

Tabara, H. & Inoue, M. 1979, A&ASupp., 39, 379

Tadros, H. & Efstathiou, G. 1995, MNRAS, 276, 45

Tajima, T., Cable, S., Shibata, K., & Kulsrud, R.M. 1992, ApJ, 390, 309

Taylor, J.H. & Cordes, J.M. 1993, ApJ, 411, 674

Taylor, J.H., Manchester, R.N., & Lyne, A.G. 1993, ApJS, 88, 529

Thompson, C. 1990, *Int. Astron. Union Symp.*, 140, 127

Tribble, P.C. 1991, MNRAS, 250, 726

Turner, M.S. & Widrow, L.M. 1988, Phys. Rev. D, 37, 10

Tytler, D., Fan, X., & Burles, S. 1996, Nature, 381, 207

Vachaspati, T. 1991, Phys. Lett., 265, 258

Vallée, J.,P. 1990, ApJ, 360, 1

Waxman, E. & Miralda-Escudé, J. 1996, ApJ, 472, L89

Weinberg, S. 1972, *Gravitation and Cosmology* (Wiley & Sons, NY) p. 413

Welter, G.L., Perry, J.J., & Kronberg, P.P. 1984, ApJ, 279, 19

Zel'dovich, Y.B. & Novikov, I.D., 1975, *Relativistic Astrophysics*, (Chicago; University of Chicago Press)

Zweibel, E.G. 1988, ApJ, 329, L1